Effect of humic monomers on the adsorption of sulfamethoxazole sulfonamide antibiotic into a high silica zeolite Y: An interdisciplinary study

(Article begins on next page)

25 April 2024

Effect of humic monomers on the adsorption of sulfamethoxazole sulfonamide antibiotic into a high silica zeolite Y: An interdisciplinary study

Ilaria Braschi[a,*], Annalisa Martucci[b], Sonia Blasioli[a], Loyiso L. Mzini[a], Claudio Ciavatta[a], Maurizio Cossi[c]

[a] Department of Agricultural Sciences, University of Bologna, 40127 Bologna (Italy)

[b] Department of Physics and Earth Sciences, University of Ferrara, 44100 Ferrara (Italy)

[c] Department of Sciences and Technological Innovation, University of Eastern Piedmont A. Avogadro, 51121 Alessandria (Italy)

* corresponding author: ilaria.braschi@unibo.it; tel: +39 051 2096208; fax: +39 051 2096203

Abstract

The adsorption efficiency of a high silica zeolite Y towards sulfamethoxazole, a sulfonamide antibiotic, was evaluated in the presence of two humic monomers, vanilin and caffeic acid, representative of phenolic compounds usually occurring in water bodies, owing their dimension comparable to those of the zeolite microporosity. In the entire range of investigated pH (5-8), adsorption of vanillin, as a single component, was reversible whereas it was irreversible for sulfamethoxazole. In equimolar ternary mixtures, vanillin coadsorbed with sulfamethoxazole, conversely to what observed for caffeic acid, accordingly to their adsorption kinetics and pKa values. Lower and higher adsorptions were observed for sulfamethoxazole and vanillin, respectively, than what it was observed as single components, clearly revealing guest-guest interactions. An adduct formed through H-bonding between the carbonyl oxygen of vanillin and the heterocycle NH of sulfamethoxazole in amide form was observed in the zeolite pore by combined FTIR and Rietveld analysis, in agreement with Density Functional Theory calculations of the adduct stabilization energies. The formation of

similar adducts, able to stabilize other naturally occurring phenolic compounds in the microporosities of hydrophobic sorbents, was proposed.

Keywords: Sulfonamides, phenols, FTIR, Rietveld refinement, DFT calculations, Amide-imide tautomerism.

1. Introduction

The release of antibiotics in the environment has been associated to chronic toxicity and the onset of the antibiotic resistance phenomena in bacteria (Gao et al., 2012). For these reasons, the removal of antibiotics from water bodies has become a public health issue which should be urgently addressed. Sulfonamides (sulfa drugs) were the first group of synthetic antimicrobials systematically used to treat/prevent bacterial infections. (Sweetman, 2011). Due to the beneficial effect on production efficiency in poultry and swine, sulfonamides are usually administrated as growth promoters in livestocks (Dibner and Richards, 2005; Neu and Gootz, 1996). Owing to their pH-dependent anionic nature, sulfonamides accumulate in water bodies, being neither completely retained by soils (Pan and Chu, 2016) nor by activated sludge in biological treatment plants (Manaia et al., 2016). Sulfamethoxazole (SMX) is one of the top-selling sulfonamide antibiotic used in human and veterinary therapy. Several studies report about its occurrence in aquatic ecosystems such as surface and drinking water, as well as wastewater treatment plants and hospital effluents (Kummerer, 2001; Brown et al., 2006; Tamtam et al., 2008; Watkinson et al., 2009). Above all, hospital and breeding farm outputs represent point source pollution which requests special consideration.

High silica (HS) zeolites have been recently tested to remove pharmaceutical from waters (de Ridder et al., 2012; Martucci et al., 2012; Grieco and Ramarao, 2013). In this contest, several model studies have indicated HS zeolites to quickly remove high amount of sulfonamide

antibiotics from water (Braschi et al., 2010; Fukahori et al., 2011; Braschi et al., 2013; Blasioli et al., 2014; Martucci et al., 2014) and to be easily regenerated (Leardini et al., 2014). Possible effect of dissolved organic matter (DOM), naturally present in water bodies, on sulfonamide adsorption into these zeolites has been ruled out, owing to the dimensions of its main components which are higher than those of the zeolite microporosities (Braschi et al., 2010), but no investigation on the effect of organic components of molecular size comparable with their pore window diameter has been addressed. This aspect is of utmost importance in order to exploit the zeolite microporosities to reduce the sulfonamide point source pollution as breeding farm effluents.

Natural and wastewaters contain plenty of low molecular weight organic molecules (Hem, 1987; Kordel et al., 1997). Among them, the phenolic component, which is formed by compounds like catechol, caffeic, ferrulic, and *p*-coumaric acids, as well as *p*-hydroxybenzaldehyde, vanillin, and other more, can be simultaneously found. The tendency of these compounds to aggregate through biotic and abiotic oxidative coupling in soils to form humic substances, where their chemical structures can be resembled, is the reason for calling them humic monomers (Nyanhongo et al., 2006; Tossel, 2009; Nuzzo and Piccolo, 2013). Due to the different structure of phenolic compounds and their coexistence in natural water compartments (Muscolo et al., 2013), two of them were identified as a model to evaluate their effect on the adsorption of sulfonamide antibiotics into a HS zeolite Y and, of more general knowledge, their ability to clog eventually the microporosities of siliceous hydrophobic sorbents. Vanilin and caffeic acid were selected as representative of humic monomers because of their different chemical nature (an aldehyde the former and an hydroxycinnamic acid the latter) and reactivity in water. Their adsorption competition against SMX, as a sulfonamide antibiotic model, was tested into a large pH range to embrace that of natural, artificial and wastewaters.

2. Materials and Methods

2.1. Chemicals

Sulfamethoxazole (4-amino-*N*-(5-methylisoxazol-3-yl)-benzenesulfonamide, SMX), was obtained from Dr. Ehrenstofer GmbH (Germany) with 99% purity. Vanillin (4-hydroxy-3-methoxybenzaldehyde, VNL) and caffeic acid (3-(3,4-dihydroxyphenyl)-2-propenoic acid, CA) were supplied by Sigma Aldrich Co LLC (USA) with 95 and 99% purity, respectively. Their chemical structures and *pKa* values are reported in Table 1.

TABLE 1

The water solubility of SMX and the two phenols at room temperature (RT) was determined by adding each compound to MilliQ water in amount exceeding that required to saturate the solution. The suspensions were sonicated (15 min) and filtered at 0.45µm (Durapore$^{®}$ membrane filters) to eliminate undissolved particles. The solubility measured by HPLC was 203±2.7 µM for SMX, 9.46±1.03 and 2.53±0.31 mM for VNL and CA, respectively.

HS zeolite Y with $SiO_2/Al_2O_3 = 200$ and surface area of 750 m^2 g^{-1} was purchased from Tosoh Corporation (Japan).

In the experiments conducted in the presence of zeolite, the desidered pH values were achieved and kept constant by addition of 0.1 N HCl/NaOH to avoid any possible coadsorption of buffering components. The pH was controlled for the entire duration of the trial.

2.2. Persistence of humic monomers in water

Aqueous solutions of VNL or CA (50 µM each) were prepared in polyallomer centrifuge tubes (Nalgene, NY, USA) dissolving the compounds in media buffered at pH 5 and 6 (10 mM CH$_3$COONa, Carlo Erba Reagents, Milano, Italy) and at pH 7 and 8 (10 mM Na$_2$HPO$_4$,

Carlo Erba Reagents, Milano, Italy). The persistence of the two phenols was followed over 48 h at RT by HPLC. Each experiment was conducted in triplicate.

2.3. Adsorption kinetics

Several aliquots of zeolite Y (1 mg) pre-equilibrated at the desired pH in the 5-8 range were placed into polyallomer centrifuge tubes where 2 mL of SMX, VNL or CA solutions (50 μM each) at the same pH were added. The suspensions were then placed on a horizontal shaker at RT and, at different times, the supernatants were separated from the pellet by centrifugation and analyzed by HPLC. To guarantee the pH stability, the pH of each suspension was checked and eventually adjusted by a few drops of 10mM HCl/NaOH solution for the entire experiment duration. The experiment was conducted in duplicate.

2.4. Adsorption-Desorption isotherms

Adsorption isotherms of SMX or VNL on zeolite Y were performed at RT in the 5-8 pH range (zeolite:solution = 1mg:2ml). Each suspension was shaken for 1 h, then centrifuged and the supernatants analyzed by HPLC. The pH of the suspensions was monitored and adjusted during the entire experiment.

Owing to the high SMX adsorption capacity of zeolite Y and the low SMX solubility at RT (203±2.7 μM), the isotherm data points at high concentrations were obtained as described in Blasioli et al. (2014). The desorption trials were conducted with the dilution method as reported in Blasioli et al. (2014). All adsorption-desorption experiments were conducted in duplicate.

The concentration of antibiotic and humic monomers in aqueous phase at equilibrium was expressed as Ce (μM) whereas the amount adsorbed by the zeolite, expressed as Cs (μmol g zeolite^{-1}), was calculated by the difference between the initial and final concentrations.

2.5. Adsorption screening

Solutions containing SMX, VNL or CA (50 µM each), and their possible combinations (binary solutions - SMX+VNL or SMX+CA - and ternary solution - SMX+VNL+CA) were prepared at different unbuffered pH values in the range 5-8. The adsorption screening was performed at RT (zeolite:solution = 1mg:2 ml). The suspensions were shaken for 1 h then centrifuged and the supernatants analyzed by HPLC. The adsorbed amount of each compound was calculated by the difference between initial and final concentration.

2.6. FT-IR spectroscopy

Harmonic vibrational frequencies were computed for SMX and VNL in their Density Functional Theory (DFT) optimized geometry (*vide infra*), and compared to experimental IR spectra.

Experimental infrared spectra were collected on a Tensor27 spectrometer (Bruker, MA, USA) with 4 cm^{-1} resolution. Self-supporting pellets (10 mg each) of zeolite Y, singly loaded with SMX or VNL and with their mixture, were obtained with a mechanical press (SPECAC, UK) at ca. 7 tons cm^{-2} and placed into an IR cell equipped with KBr windows permanently attached to a vacuum line, allowing sample dehydration *in situ*. FTIR spectra of SMX or VNL in CH_2Cl_2 were performed in a NaCl cell for liquids. Spectrum of the bare zeolite were collected as a control.

2.7. X-ray Powder Diffraction

X-ray powder diffraction (XRPD) data were collected on a Bruker D8 Advance Diffractometer equipped with a Sol-X detector, using Cu $K_{\alpha1,\alpha2}$ radiation. The spectra were measured in the 3°-110° 2Θ range with a counting time of 12 s step^{-1}. All the structure refinements were performed by using the Rietveld method (EXPGUI version of GSAS (Toby, 2001)) in the *Fd-3* space groups. The crystal data and refinement details are summarized in the Supplementary Materials (see Table 1S).

The structures in Figure 4 were generated using the VESTA software package (Momma and Izumi, 2011).

2.8. Chromatographic analysis

Concentrations of SMX, VNL, and CA were determined by HPLC-Diodarray analysis (Jasco, Japan) set at 267, 231, and 324 nm, respectively, equipped with a 4.60 nm x 250 mm Waters Spherisorb® 5µm C8 analytical column (Waters, USA) kept at 35 °C into a column oven (Jones Chromatography model 7971) and eluted with acetonitrile:water (30:70 by volume, pH 2.7 for H_3PO_4, flow rate 1 ml min^{-1}). Under these conditions, the retention times were 6.8, 5.5, and 3.8 min for SMX, VNL, and CA, respectively.

2.9. DFT calculations

All the calculations were performed at the DFT level with B3LYP density functional (Becke, 1988; 1993), the most popular hybrid density functional for molecular structure optimization and vibrational spectra simulation: the B3LYP performances for this kind of applications have been recently reviewed (Kovacs et al., 2015). Different basis sets, both double- and triple-ζ (cc-pVDZ and cc-PVTZ) were used for geometry optimizations, and energy and frequency calculations; in the zeolite cage model, Si atoms were assigned Hay and Wadt (LANL2) effective core potential and basis set (Hay and Wadt, 1985a,b; Wadt and Hay, 1985). Dispersion energy corrections were included through the semiempirical approach proposed by Grimme and implemented in Gaussian09 (GD3 procedure) (Grimme et al., 2010). The Y zeolite cage was modeled by extracting a suitable cluster from the database periodic structure as described e.g. in Braschi et al. (2012).

3. Results and discussion

Freshwater lakes, ponds and streams usually have a pH of 6-8 depending on the surrounding soil and bedrock (http://geology.com/rocks). For this reason, all the adsorption experiments

were conducted in the 6-8 pH range in order to evaluate the effect of water pH on possible adsorption of SMX, VNL, and CA by the zeolite. For sake of completeness, pH 5 was considered as well, due to the acidic nature of the investigated compounds which are likely to be better retained by the sorbent under acidic conditions.

To rule out the degradation of the humic monomers within the time duration of adsorption trials, their persistence in buffered water was firstly evaluated. The degradation kinetics of VNL and CA in the 5-8 pH range is reported in the Supplementary Materials (see Figure 1S). The concentration of VNL remained constant within 24 h in the entire range of the investigated pHs whereas CA concentration unchanged in the 5-7 pH range. At pH 8, CA was transformed with a half-life time of 48 h into two degradation products. Since the effect of basic pHs on the abiotic oxidation mechanism of CA is well-known (Cilliers and Singleton, 1989), the identification of the byproducts was considered beyond the scope of this study. As shown in the inset of Figure 1S(b), CA concentration could be considered constant up to 1 h (~2% was transformed), thus safely allowing the investigation of its adsorption for short contact times (adsorption equilibrium of sulfonamides into this zeolite within a few minutes (Braschi et al., 2010; Blasioli et al., 2014).

3.1. Adsorption trials

In the light of the observations described above, the adsorption kinetics of SMX, VNL, and CA on zeolite Y were followed within 1 h contact as shown in Figure 2S. The SMX adsorption equilibrium was favourable in the entire range of pH investigated: the equilibrium was reached within 1 min and the amount retained by the zeolite was inversely related to the pH of water solutions. These findings can be explained considering the hydrophobic nature of the sorbent and pH-dependent nature of SMX.

The hydrophobicity of zeolites is inversely related to the content of extraframework cations counterbalancing the isomorphic substitution of Al^{3+} for Si^{4+} in the framework and to the

content of defects (silanol groups) in the framework (Kawai and Tsutsumi, 1992). The high SiO_2/Al_2O_3 ratio (200) and the low content of H-bonded silanols (24 SiOH per Y unitary cell, Braschi et al., 2010) make the selected zeolite Y a hydrophobic material as proved by its low water content when air dried (ca. 1% dw).

As far as the affinity of SMX for the hydrophobic zeolite is concerned, the adsorption is favoured when the antibiotic molecule is in associated form (*pKa* 5.7, Table 1). Therefore, the SMX affinity was in the order: pH 5 (SMX mainly in neutral form) > pH 6 (both neutral and anionic forms) > pH 7 (mainly anionic form) > pH 8 (anionic form).

The adsorption equilibrium of CA at pH 5 was reached within 15 min, whereas at higher pH values no visible adsorption was found within 1 h. The CA *pKa* of 4.5 could explain its scarce affinity for the zeolite in that in the entire pH investigate, the negative form of CA predominate. For VNL, the adsorption equilibrium was reached in 1 min over the entire range of pH, making thus its adsorption competitive with SMX for the zeolite adsorption sites, although the retained amount was significant only in the 5-7 pH range. At pH 8, only a limited amount of VNL was retained by the zeolite as expected by its *pKa* value (7.4) due to the occurrence of species mainly in anionic form.

In the following, only the adsorption-desorption isotherms of SMX and VNL are reported owing to the negligible adsorption of CA in the investigated pH range.

As shown in Figure 1A, the maximal adsorption of SMX at pH 5-6 was similar and attested at *ca.* 22% of zeolite dry weight (dw) whereas at pH 7 and 8, the plateau was reached at 3.3 and 1.5% zeolite dw, respectively.

FIGURE 1

As clearly shown by the curves slope at low concentrations, the affinity for the zeolite is inversely related to the pH of the solution. As already detailed, the antibiotic pK_a value (5.7, Table 1) can explain both the higher affinity and loading at acidic pH values. Considering the

number of cages contained in 1 g zeolite (4.2×10^{20}, Braschi et al., 2010) and the antibiotic molecules adsorbed at pH 5-6 (5.3×10^{20} on average), the presence of at least one molecule per cage could be calculated, whereas a partial loading was achieved at pH 7 and 8 (20 and 9% of cages embeds one SMX molecule, respectively). The SMX adsorption reversibility was investigated only at pH 7 and 8, being the adsorption at acidic pH already defined irreversible (Blasioli et al., 2014). As shown in the detail, both the SMX desorption isotherms at pH 7-8 run parallel to the x-axis, thus indicating an irreversible adsorption at neutral-basic pH values as well.

Figure 1B shows the adsorption isotherms of VNL on the zeolite in the pH range of 5-7 owing to its negligible adsorption at pH 8. The VNL adsorption curves resemble an "S" type (Giles et al., 1960), also known as a "cooperative" adsorption. According to the model, the affinity of the adsorbate for the sorbent increases by increasing the retained amount due to an extrastabilization among guest species by interactions with those previously adsorbed, as well as with the sorbent. The plateau concentration was inversely related to the water pH and attested at ca. 13 and 8% zeolite dw at acidic and neutral pH, respectively. At acidic pHs, a full occupancy of the zeolite cages was found whereas 75% of cages were occupied at pH 7. As the desorption curves (see detail in Figure 1B) overlapped to the adsorption ones at any investigated pH, the VNL adsorption was defined fully reversible, in accordance to its solubility (9.46 mM at RT and pH 6).

As far as the possible effect of the humic monomers on SMX retention by the zeolite is concerned, Table 2 reports an adsorption screening conducted in aqueous solutions containing different combinations of the investigated compounds at equimolar concentrations.

TABLE 2

The adsorption of SMX and VNL, as single components, decreased at increasing pH in accordance to their *pKa*. For SMX, a similar adsorption profile as a function of pH has been already reported for a zeolite Y with a $SiO_2/Al_2O_3 = 100$ (Fukahori et al., 2011), thus highlighting a similar affinity for the antibiotic in the 100-200 range of SiO_2/Al_2O_3 ratio. In our study, the adsorption of SMX was ca. threefold that of VNL in the entire pH range, with the exception of pH 8, where only SMX was retained by the zeolite. As a single component, CA adsorbed in low amount at pH 5 whereas it was not retained at higher pH values.

When binary mixtures of SMX+VNL were contacted with the zeolite, a coadsorption of both compounds was observed in agreement with their comparable and fast kinetics (<1 min, Figure 2S). In the entire range of pH, the SMX amount retained in the presence of VNL was found reduced with respect to what it was observed as a single component. On the contrary, VNL adsorption was found higher in the presence of SMX than as a single component, thus highlightening possible interactions with SMX into the zeolite pores (*vide infra*). Interestingly, at pH 8 which is a pH common to most part of natural surface waters, the embedded amount of VNL and SMX was comparable (14.7 and 12.2% of initial concentration, respectively). According to the *pKa* value of VNL with respect to SMX (7.4 and 5.7, respectively), VNL adsorption should be favoured at all the pH values. Likely, the lower SMX solubility, besides its bulky structure that maximizes the van der Waals interactions with the pore wall (Blasioli et al., 2014), favours its adsorption with respect to VNL.

When binary mixtures of CA and SMX were exposed to the zeolite, no significant amount of CA was retained in the entire range of investigated pHs, whereas SMX showed an adsorption profile resembling that observed as a single component. These findings can be explained by the lower pK*a* of CA with respect to SMX (4.5 and 5.7, respectively), besides its higher solubility (2.53 mM and 203 μM respectively).

The adsorption trend observed for the binary mixtures (VNL+SMX and CA+SMX) was confirmed when ternary mixtures of SMX+VNL+CA were contacted with the zeolite: only a simultaneous adsorption of SMX and VNL was observed.

3.2 Host-guest interactions between VNL and HS zeolite Y

To maximize the host-guest interactions, a zeolite sample loaded with VNL at 13.2% zeolite DW was investigated by IR analysis combined to Rietveld structure refinement of XRPD data. This allowed a better observation of the spectral features of the adduct eventually formed.

In Figure 3A, experimental FT-IR spectra of VNL in CH_2Cl_2 and singly embedded into the zeolite Y are reported, along with the harmonic vibrational spectrum calculated by the DFT level for the isolated molecule (in vacuo). In the spectrum in CH_2Cl_2, although strong solvent bands in the 3250-2750 and 1500-1400 cm^{-1} range are overlapped to those of VNL, as well as the occurrence of signals coming from water traces in the region above 3600 cm^{-1}, the most part of VNL vibrations could be observed.

FIGURE 3

The assignment of the main absorptions was done by comparing the values calculated in vacuo to the experimental ones as reported in Table 3. Here, the computed harmonic frequencies are systematically overestimated with respect to the corresponding experimental absorption but the spectral pattern was reproduced accurately enough to allow the interpretation.

Noteworthy, the structure of VNL computed in vacuo is organized through an intramolecular five-membered ring whith the OH group H-bonded to the methoxyl oxygen atom (νPhO-H at 3751 cm^{-1}). The same arrangement was also hypothesized in both CH_2Cl_2 and when embedded into the zeolite (νPhO-H at 3518 and 3528 cm^{-1}, respectively) owing to the nonpolar character of the solvent and the zeolite pore wall. The similar position of the other

VNL bands in both environments confirmed the solvating effect of zeolite on the guest molecule. These features indicate that the interactions between VNL and the zeolite framework are due to weak dispersive forces whose contributions are strong enough to stabilize the intramolecular H-bonded VNL into the cage.

Rietveld refinement performed on the VNL-loaded zeolite revealed the presence of about 9.5 molecules per unit cell (corresponding to 11% zeolite dw and 1.18 molecules/cage), in good agreement with the loading data (13.3% zeolite dw). These molecules are hosted in the Y cage in crystallographic sites partially statistically occupied (C1, C2, and C3 sites in Figure 4S in the Supplementary Materials). These molecules show the aromatic ring (C1 site) in the window that joins together neighbouring cages as shown in Figure 4A.

FIGURE 4

They can assume six different orientations which are identical and related by a rotation of 60º about c or by a mirror operation perpendicular to c (Figure 4S in the Supplementary Materials). The C2/C3 sites can be alternatively occupied by carbon or oxygen atoms, because the molecule symmetry is lower than Fd-3. The methoxylic group is given by C2 (when hosting oxygen) and C3 (when hosting CH_3), the carbonyl group is given by C2 (when hosting carbon) and C3 (when hosting oxygen), and finally the hydroxyl group is given by C2 (when hosting oxygen and C3 site is empty) (Figure 4S).

The formation of more distorted wide-open apertures upon VNL adsorption is likely associated to the observed relative expansion of the framework thus explaining the increase of the unit cell parameters and the cell volume expansion (Table 1S).

Consequently, the Crystallographic Free Areas (C.F.A.) increased (42.61 Å^2) when compared with the bare material (39.07 Å^2). Variations of ellipticity (ε) (defined as the largest/shortest oxygen-oxygen distances) of the 12MR apertures after organic molecules adsorption are also reported (ε =1.06 and 1.02 in Y-VNL and Y, respectively).

Owing to the full reversibility of the adsorption process (Figure 2), the refined distances can be ascribed to weak dispersive forces acting between the VNL methoxyl/oxydryl oxygens (C2 site), as well as the methyl group or the carbonyl oxygen (C3), and the zeolite framework.

3.3. Guest-guest interactions between SMX and VNL embedded into the HS zeolite Y

To maximize the possible guest-guest interactions into the zeolite pores, a Y sample simultaneously loaded with SMX and VNL (6.9 and 20.1% zeolite dw, respectively) was investigated by infrared and Rietveld analysis. In the sample, 100% of pores contained at least one SMX molecule whereas ca. 50% embedded one VNL molecule on average.

The experimental IR spectrum of the SMX+VNL loaded mixture is reported in Figure 3B. Here, spectra of singly loaded SMX or VNL are reported for comparison. A detailed description of the host-guest interactions developed by SMX embedded into the same zeolite in amide form has been already addressed (Blasioli et al., 2014).

In the spectrum of the loaded SMX-VNL mixture (Figure 3B), the occurrence of bands at position similar to those of the singly embedded compounds can be resembled. As far as the VNL contributions are concerned, a clear perturbation of the carbonyl stretching region could be observed between 1700 and 1650 cm^{-1}, thus indicating this group likely involved in the stabilization of a SMX-VNL cluster. Concerning the SMX signals, the bands of singly embedded SMX (ca. 50%) are found overlapped to contributions of those clusterised with VNL (remaining 50%) and a clear perturbation of the stretching and bending NH signals was observed. In clusterised SMX, the stretching of NH at 3193 cm^{-1} is downshifted (Δ = -47 cm^{-1}) with respect to its position when singly adsorbed (3240 cm^{-1}), whereas the NH bending at 1626 cm^{-1} is upshifted (Δ = +5 cm^{-1}) with respect to that as a single component (1621 cm^{-1}). These findings clearly indicates an H-bonding between the VNL carbonyl and the SMX NH (VNL-C=O···HN-SMX), with the latter group which can be originated from both (i) SMX in

amide form (SO$_2$-NH-) and (ii) the heterocycle ring NH of SMX in imide form (SO$_2$-N=C). Unfortunately, the computed stretching of the SMX heterocycle NH is overlapped (3563 cm^{-1}) to that of the amide SO$_2$-NH (3565 cm^{-1}) thus making impossible any assignment of the signal experimentally found at 3193 cm^{-1}.

The XRPD pattern collected on Y-SMX-VNL, and compared to Y-VNL and Y-SMX samples, showed differences in the intensity of the diffraction peaks, with the most significant been associated to the low 2θ angle region (Figure 3S in the Supporting Materials), related to both the extraframework species nature and distribution.

Only small changes in the cell parameters of Y-SMX-VNL occur with respect to Y-VNL sample; in particular, a slight decrease of *a* and cell volume parameters are observed (Table 1S). The Y-SMX-VNL refinement revealed the presence of 4 VNL and 10 SMX molecules per unit cell (ca. 7 and 20% zeolite dw, respectively, and ca. 0.5 and 1 molecule per cage, respectively). According to Blasioli et al. (2014), SMX molecules singly loaded are almost at the center of the supercage with its plane perpendicular to the threefold axes of the unit cell, whereas the isoxazole ring is found with six different orientations (see Figure 4B). In the Y-SMX-VNL sample (Figure 4C), the SMX aniline ring (C1 site) is situated in the window that joins neighboring supercages. The SMX isoxazole and aniline rings form a typical "V" configuration with the torsion angle S-N2-C7 of about 125.7°, with respect to that (126.0°) refined after adsorption of SMX as a single component (Blasioli et al., 2014).

As far as concerns coadsorbed VNL molecules, they can assume the six different orientations related by a rotation of 60º about *c* which are identical to those observed after adsorption of VNL as a single component (Figure 4A), with the aromatic ring in C1 site, and C2/C3 sites which can be alternatively occupied by carbon or oxygen atoms, as already reported for the Y-VNL system. The 12MR apertures became more distorted (ε=1.08), consequently the C.F.A. is larger (42.25 Å^2) when compared with the as-synthesized material (39.07 Å^2).

The refined bond distances between VNL and SMX in the cluster highlighted that interactions occur between these two species, in keeping with the data of FT-IR analysis. In particular, as shown in Figure 4C, the distance between C2 site of VNL (carbonyl oxygen) and the SMX heterocycle ring N (N-C2=2.98(4) Å) indicates the interaction between the VNL carbonyl oxygen and the SMX heterocycle ring nitrogen as the most likely, whereas the nitrogen of the S-N-C moiety (amide form) can also interact but at higher interaction distance (3.04(4) Å, Figure 4C). These results confirmed the occurrence of an H-bonding between the VNL carbonyl group and SMX NH, thus indicating the SMX imide form clusterised to VNL. DFT calculations could help to quantify the guest-guest interaction energy both for isolated SMX-VNL adducts and after embedding in Y zeolite. The addition energy in vacuo was computed at the B3LYP/cc-pVDZ level including Grimme's dispersion energy and the counterpoise correction to the BSSE (Boys and Bernardi, 1970), resulting -14.9 kcal/mol for the SMX imide form and -9.2 kcal/mol for the amide isomer, thus confirming the Rietveld findings. The optimized structures of the two adducts are reported in Figure 5.

FIGURE 5

The adduct with imide SMX was then embedded in the Y cage model and re-optimized at the same level (LANL2DZ effective core potentials were used for Si atoms): the final structure is shown in Figure 5; besides the SMX-VNL NH-O bond already observed in vacuo, two other hydrogen bonds establish between the SMX amine group and a cage oxygen and between the cage silanol group and one sulfonamide oxygen. For the embedded cluster the interactions with the zeolite cage override the guest-guest interactions: in fact, SMX and VNL are strongly distorted inside the cage, so that the addition energy with respect to the isolated molecules is +2.9 kcal/mol, but when the interactions with the cage are added, the total energy with respect to the isolated fragments becomes -56.2 kcal/mol. Such a host-guest

interaction is largely dominated by the dispersion contribution, computed through Grimme's atom-atom approach.

Conclusions

The effect of two model molecules of humic monomers (vanillin -VNL - and caffeic acid - CA) on the adsorption of sulfamethoxazole (SMX) by a high silica zeolite Y was assessed in batch solution within a large range of pH. The adsorption of VNL as a single component was kinetically favourable (<1 min), pH-dependent in accordance to its weak acidic character (*pKa* 7.4), and reversible at any pH. On the contrary, CA adsorption was always unfavoured owing to its higher acidity (*pKa* 4.5). The adsorption of SMX was also pH-dependent (*pKa* 5.4) but irreversible at all the pH values considered, due to its bulky "V" structure which stabilizes the embedded molecule. A SMX and VNL simultaneous adsorption was observed when the zeolite was exposed to their equimolar mixture: the formation of a bulky 1:1 SMX-VNL cluster into the zeolite pores explained their different (lower and higher, respectively) loading from what it was observed as single compounds. As defined by infrared analysis combined to Rietveld refinement, the adduct formed into the zeolite pore through an H-bonding between the heterocycle NH of SMX in amide form and the carbonyl oxygen of VNL, with a stabilization energy, computed in vacuo at DFT level, of -56.2 kcal/mol with respect to the isolated molecules. The formation of similar adducts with sulfonamide antibiotics, all bearing an heterocycle nitrogen able to stabilize other humic phenolic monomer into the zeolite micropores, can be hypothesized.

In addition and of more general meaning, according to our results on model molecules, humic monomers do not seem involved *per se* in the pore clogging of the zeolite, since derivatives of phenols (as vanillin) can be released by the hydrophobic porosities of the zeolite whereas the more acidic hydroxycinnamic acids (as caffeic acid) are not retained at all. These findings

are of certain interest for scientists working with zeolite-based technologies to treat natural and wastewaters where a variety of humic phenolic compounds always occur.

References

Becke, A.D., 1988. Density-functional Exchange-energy Approximation with Correct Asymptotic Behavior. Phys. Rev. A. 38, 3098-3100.

Becke, A.D., 1993. Density Functional Thermochemistry. III. the Role of Exact Exchange. J. Chem. Phys. 98, 5648-5652.

Blasioli, S., Martucci, A., Paul, G., Gigli, L., Cossi, M., Johnston, C.T., Marchese, L., Braschi, I., 2014. Removal of sulfamethoxazole sulfonamide antibiotic from water by high silica zeolites: A study of the involved host–guest interactions by a combined structural, spectroscopic, and computational approach. J. Coll. Interf. Sci. 419, 148-159.

Boys, S.F., Bernardi, F., 1970. The calculation of small molecular interactions by the differences of separate total energies. Some procedures with reduced errors. Mol. Phys. 19, 553-566.

Braschi, I., Blasioli, S., Gigli, L., Gessa, C.E., Alberti, A., Martucci A., 2010. Removal of sulfonamide antibiotics from water: Evidence of adsorption into an organophilic zeolite Y by its structural modifications. J. Hazard. Mat. 178, 218-225.

Braschi, I., Gatti, G., Bisio, C., Berlier, G., Sacchetto, V., Cossi, M., Marchese, L., 2012. The role of silanols in the interactions between methyl *ter*-butyl ether and high-silica faujasite Y: An infrared spectroscopy and computational model study. J. Phys. Chem. C 116, 6943-6952.

Braschi, I., Paul, G., Gatti, G., Cossi, M., Marchese, L., 2013. Embedding monomers and dimers of sulfonamide antibiotics into high silica zeolite Y: an experimental and computational study of the tautomeric forms involved. RSC Advances 3, 7427-7437.

Brown, K.D., Kulis, J., Thomson, B., Chapman, T.H., Mawhinney, D.B., 2006. Occurrence of antibiotics in hospital, residential, and dairy effluent, municipal wastewater, and the Rio Grande in New Mexico. Sci. Total Environ. 366, 772-783.

Cilliers, J.J.L., Singleton, V.L., 1989. Nonenzymic autoxidative phenolic browning reactions in a caffeic, acid model system. J. Agric. Food Chem. 37, 890-896.

Colthup, N.B., Daly, L.H., Wiberley, S.E., Editors. 1990. In Introduction to Infrared and Raman spectroscopy. Third Edition, Academic Press, USA, pp 261-266.

de Ridder, D.J., Verberk, J.Q.J.C., Heijman, S.G.J., Amy, G.L., van Dijk, J.C., 2012. Zeolites for nitrosamine and pharmaceutical removal from demineralised and surface water: Mechanisms and efficacy. Sep. Purif. Tech. 89, 71-77.

Dibner, J.J., Richards, J.D., 2005. Antibiotic growth promoters in agriculture: History and mode of action. Poultry Sci. 84, 634-643.

Fukahori, S., Fujiwara, T., Ito, R., Funamizu, N., 2011. pH-Dependent adsorption of sulfa drugs on high silica zeolite: Modeling and kinetic study. Desalination 275, 237-242.

Gao, P., Munir, M., Xagoraraki, I., 2012. Correlation of tetracycline and sulfonamide antibiotics with corresponding resistance genes and resistant bacteria in a conventional municipal wastewater treatment plant. Sci. Total Environ. 421–422, 173-183.

Giles, C.H., MacEwan, T.H., Nakhwa, S.N., Smith, D., 1960. Studies in adsorption: Part XI. A system of classification of solution adsorption isotherms, and its use in diagnosis of adsorption mechanisms and in measurement of specific surface areas of solids. J. Chem. Soc. 111, 3973-3993.

Grieco, S.A., Ramarao, B.V., 2013. Removal of TCEP from aqueous solutions by adsorption with zeolites. Colloids and Surfaces A: Physicochem. Eng. Aspects 434, 329-338.

Grimme, S., Antony, J., Ehrlich, S., Krieg, H., 2010. A consistent and accurate *ab initio* parametrization of density functional dispersion correction (DFT-D) for the 94 elements H-Pu. J. Chem. Phys. 132, 154104-154119.

Hem, J.D., 1987. Study and interpretation of the chemical characteristics of natural water. 3rd Edition, U. S. Geological Survey Water-Supply Paper 2254, United States Governement Printig Office.

Hay, P.J., Wadt, W.R., 1985a. *Ab initio* effective core potentials for molecular calculations. Potentials for the transition metal atoms Sc to Hg. J. Chem. Phys. 82, 270-283.

Hay, P.J. Wadt, W.R., 1985b. *Ab initio* effective core potentials for molecular calculations. Potentials for K to Au including the outermost core orbitals. J. Chem. Phys. 82, 299-310.

Kawai T., Tsutsumi K., 1992. Evaluation of hydrophilic-hydrophobic character of zeolites by measurements of their immersional heats in water. Colloid Polym Sci 270, 711-715.

Kiss, T., Nagy, G., Pécsi, M., Kozlowski, H., Micera, G., Erre, L.S., 1989. Complexes of 3,4-dihydroxyphenyl derivatives—X. Copper(II) complexes of chlorogenic acid and related compounds. Polyhedron, 8, 2345-2349.

Koizumi, T., Arita, T., Kakemi, K. 1964. Absorption and excretion of drugs. XIX: some pharmacokinetic aspects of absorption and excretion of sulfonamides (1): absorption from rat stomach. Chem. Pharm. Bul. 12, 413-420.

Kordel, W., Dassenakis, M., Lintelmann, J., Padberg, S., 1997. The importance of natural organic material for environmental processes in waters and soils. Pure & Appl. Chem. 69 (7), 1571-1600.

Kovacs, A., Konings, R.J.M., Gibson, J.K., Infante, I., Gagliardi, L., 2015. Quantum chemical calculations and experimental investigations of molecular actinide oxides. Chem. Rev. 115, 1725-1759.

Kummerer, K., 2001. Drugs in the environment: emission of drugs, diagnostic aids and disinfectants into wastewater by hospitals in relation to other sources: a review. Chemosphere 45, 957-969.

Leardini, L., Martucci, A., Braschi, I., Blasioli, S., Quartieri, S., 2014. Regeneration of high-silica zeolites after sulfamethoxazole antibiotic adsorption: a combined in situ high-temperature synchrotron X-ray powder diffraction and thermal degradation study. Min. Mag. 78 (5), 1141–1159.

Manaia, C.M., Macedo, G., Fatta-Kassinos, D., Nunes, O.C., 2016. Antibiotic resistance in urban aquatic environments: can it be controlled? Appl. Microbiol. Biotechnol. 100, 1543-1557.

Martucci, A., Pasti, L., Marchetti, N., Cavazzini, A., Dondi, F., Alberti, A., 2012. Adsorption of pharmaceuticals from aqueous solutions on synthetic zeolites. Micropor. Mesopor. Mat. 148, 174-183.

Martucci, A., Braschi, I., Marchese, L., Quartieri, S., 2014. Recent advances in clean-up strategies of waters polluted with sulfonamide antibiotics: a review of sorbents and related properties. Min. Mag. 78 (5), 1115-1140.

Momma, K., Izumi, F., 2011. VESTA 3 for three-dimensional visualization of crystal, volumetric and morphology data. J. Appl. Crystallogr. 44, 1272-1276.

Muscolo, A., Sidari, M., Texeira da Silva, J.A., 2013. Biological effects of water-soluble soil phenol and soil humic extracts on plant systems. Acta Physiol. Plant 35, 309-320.

Neu, H.C., Gootz, T.D., 1996. Chapter 11 Antimicrobial Chemotherapy, in Medical Microbiology. 4th edition, Baron S., editor. Galveston (TX), University of Texas Medical Branch at Galveston.

Nuzzo, A., Piccolo, A., 2013. Enhanced catechol oxidation by heterogeneous biomimetic catalysts immobilized on clay minerals. J. Mol. Cat. A - Chemical 371, 8-14.

Nyanhongo, G.S., Rodriguez, S., Georg, M., 2006. Coupling of 2,4,6-trinitrotoluene (TNT) metabolites onto humic monomers by a new laccase from *Trametes modesta.* Chemosphere 64 (3), 359-370.

Pan, M., Chu, L.M., 2016. Adsorption and degradation of five selected antibiotics in agricultural soil. Science of the Total Environment 545–546, 48–56.

Rocks: Igneous, Metamorphic and Sedimentary in http://geology.com/rocks.

Sweetman, S., editor. 2011. The complete drug reference. London: Pharmaceutical Press.

Tamtam, F., Mercier, F., Le Bot, B., Eurin, J., Tuc Dinh, Q., Clément, M., Chevreuil, M., 2008. Occurrence and fate of antibiotics in the Seine River in various hydrological conditions. Sci. Total Environ. 393, 84-95.

The Chapman and Hall Chemical Database 1995. Chapman & Hall/CRC (UK).

Tossel, J.A., 2009. Quinone-hydroquinone complexes as model components of humic acids: Theoretical studies of their structure, stability and Visible-UV spectra. Geochim. Cosmochim. Acta 73 (7), 2023-2033.
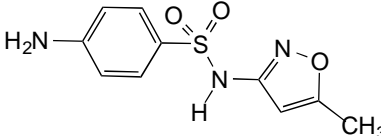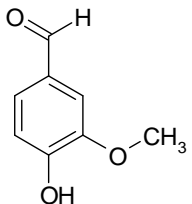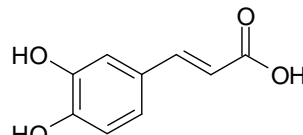
Toby, B.H., 2001. EXPGUI, a graphical user interface for GSAS, J. Appl. Cryst. 34, 210-213.

Wadt, W.R., Hay, P.J., 1985. *Ab initio* effective core potentials for molecular calculations. Potentials for main group elements Na to Bi. J. Chem. Phys. 82, 284-298.

Watkinson, A.J., Murby, E.J., Kolpin, D.W., Costanzo, S.D., 2009. The occurrence of antibiotics in an urban watershed: From wastewater to drinking water. Sci. Total Environ. 407, 2711-2723.

Table 1. Characteristics of chemicals under investigation.

Chemical name (Acronym)	Chemical structure	MW (mol g^{-1})	pK$_a$
Sulfamethoxazole (SMX)		253.3	5.7[a]
Vanillin (VNL)		152.15	7.4; 11.4[b]
Caffeic acid (CA)		180.16	4.5; 8.6; 12.5[c]

[a] (Koizumi et al., 1964); [b] (The Chapman and Hall Chemical Database, 1995); [c] (Kiss et al., 1989)

1

2 **Table 2**. Adsorption on HS zeolite Y of equimolar concentration of VNL, CA, and SMX as single components, binary and ternary mixtures at

3 different pH (1 h contact time at RT). In parenthesis the absolute error.

| | **Amount adsorbed by the HS zeolite Y as a percentage of initial concentration (50 μM)** | | | | | | | | | |
pH	*Single component*			*Binary mixture*				*Ternary mixture*		
	VNL	**SMX**	**CA**	**VNL**	**SMX**	**CA**	**SMX**	**VNL**	**SMX**	**CA**
5	34.9 (1.3)	95.6 (0.0)	3.7 (1.1)	46.0 (0.0)	93.2 (1.0)	4.7 (0.6)	93.1 (0.6)	47.2 (0.4)	96.8 (0.5)	5.1 (0.3)
6	23.5 (1.6)	88.0 (1.5)	0.5 (0.0)	36.9 (3.5)	77.9 (4.9)	4.0 (1.5)	85.4 (4.2)	37.6 (0.9)	81.0 (2.0)	4.9 (0.5)
7	21.4 (0.8)	66.1 (4.6)	0.1 (0.0)	19.7 (6.3)	45.3 (4.9)	4.0 (1.0)	62.4 (11.8)	13.6 (0.3)	39.0 (0.4)	5.0 (2.0)
8	0.0 (2.4)	26.1 (8.5)	2.9 (1.5)	12.2 (2.9)	14.7 (6.5)	1.8 (0.3)	22.6 (1.9)	6.4 (1.5)	11.8 (0.4)	0.0 (0.3)

4

1

2   **Table 3.** Main vibrational modes of vanillin calculated in vacuo and experimentally

3   determined in CH_2Cl_2 and adsorbed into the zeolite Y.

| Vibrational modes*	Vanillin		
	Computed	**In CH_2Cl_2**	**Embedded in Y**
νPhO-H	3751	3518	3524
νCH$_{Ph}$	3203-3186	not visible**	3070, 3013
νCH$_3$	3138-3016	not visible**	2943, 2824
νCH$_{aldehyde}$	2866	2733	2731
νCO$_{aldehyde}$	1758	1688	1693
νPh$_{quadrant}$ + δPhO-H	1625	1597	1595
νPh$_{sextant}$	1547	1510	1510
Def$_{out-of-phase}$ CH$_3$	1506	1464	1466
Def$_{in-phase}$ CH$_3$ + δPhO-H + δCH$_{aldehyde +}$ νPh$_{sextant}$	1467	not visible**	1437
δCH$_{aldehyde}$ + νPh$_{sextant}$	1418	not visible**	1402
δPhO-H + δCH$_{aldehyde}$ + νPh$_{sextant}$	1409	1381	1381

4   * For definition of ring vibrational modes see: Colthup and Wiberley, 1990; ** not visible
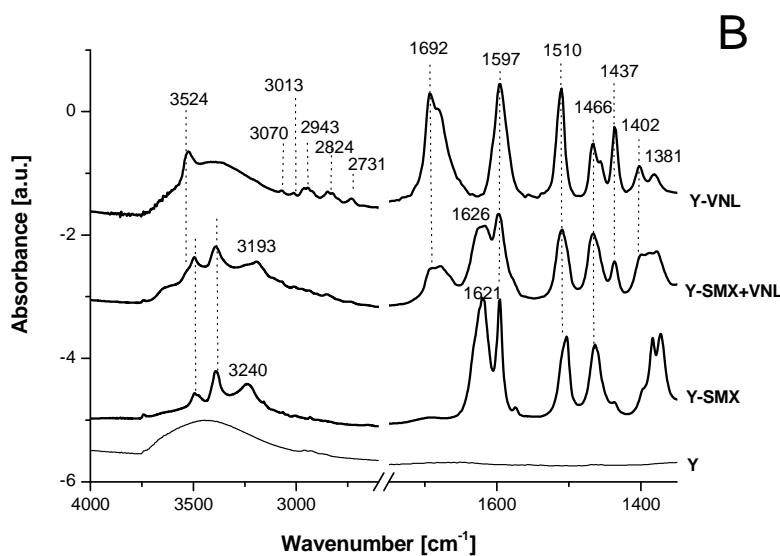
5   because overlapped to CH_2Cl_2 bands

6
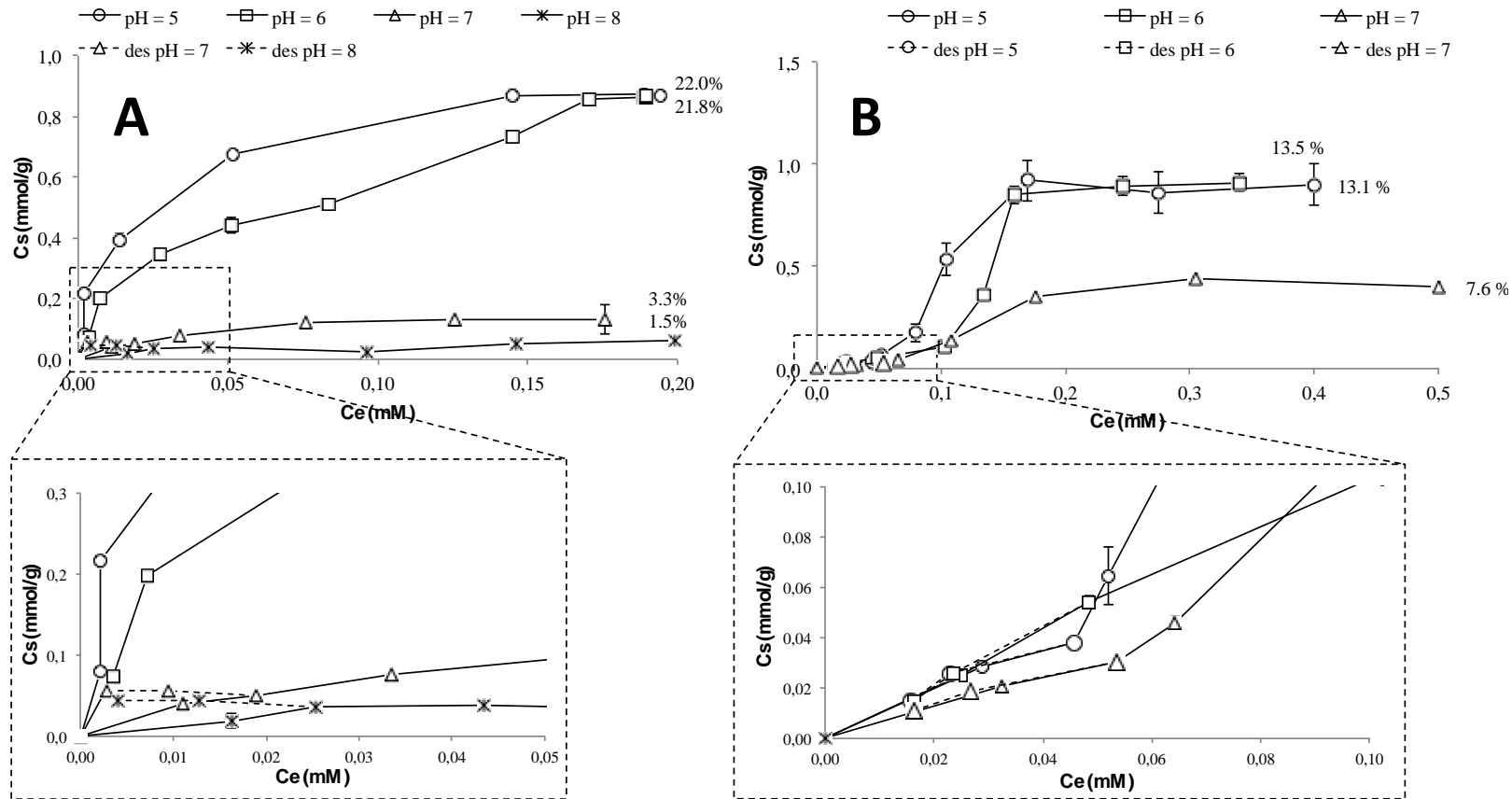
Fig. 1. Adsorption and desorption isotherms (solid and dashed lines) of (A) sulfamethoxazole and (B) vanillin by HS zeolite Y at different pH (1 h contact time at RT). A detail of isotherms is reported. Bars indicate the absolute error.
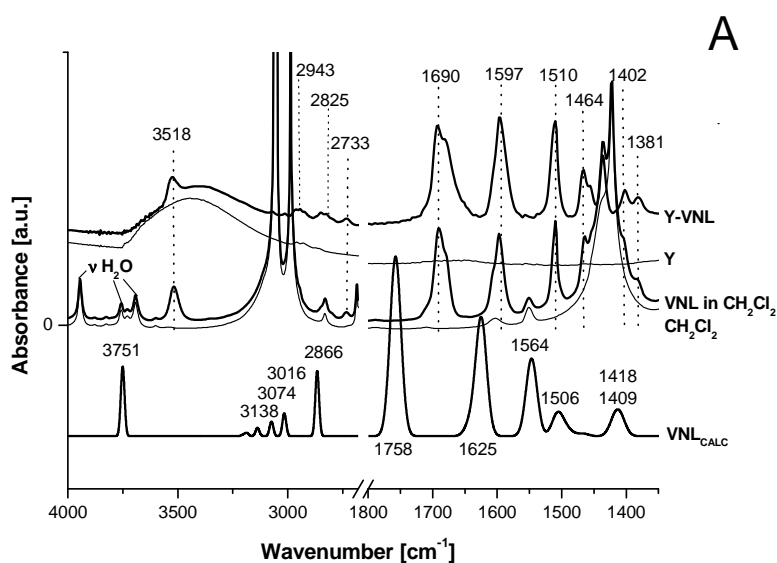
Fig. 3. A) DFT calculated spectrum of VNL in vacuo (VNL$_{CALC}$) and experimental spectra of VNL in CH$_2$Cl$_2$ and adsorbed into zeolite Y (Y-VNL). Experimental spectra of CH$_2$Cl$_2$ and zeolite Y are reported for comparison. B) Experimental spectra of the zeolite singly loaded with VNL (13% zeolite dw) or SMX (21% zeolite dw) and with a SMX+VNL mixture (7 and 20% of zeolite dw, respectively).

1

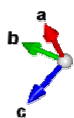2   **A**   **B**   **C**
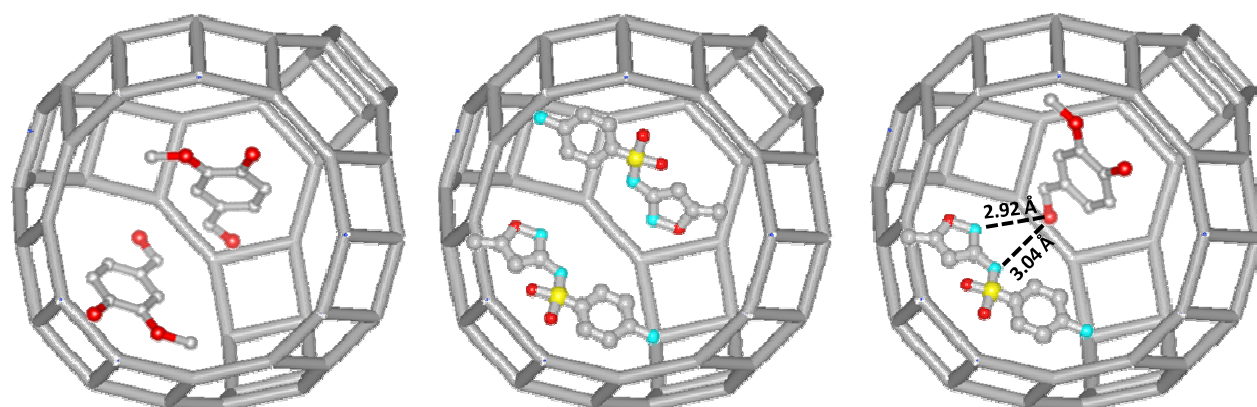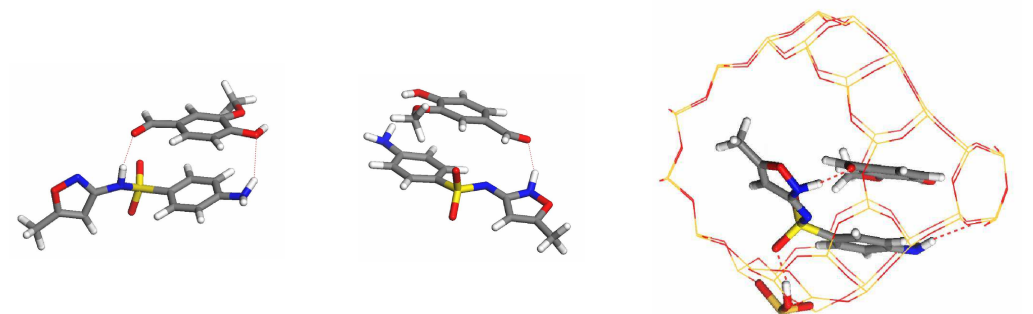
3

4   **Fig. 4**. Possible orientations of VNL (A), SMZ (B) and SMZ+VNL (C) in the zeolite Y cage

5   (O: red, N: blue, S: yellow).

6

1

2   **Fig. 5**. DFT optimized structures of SMX+VNL complex with SMX in amide (left) and

3   imide form (center) in vacuo and in the zeolite cage (right).